FPCountR: Absolute protein quantification using fluorescence measurements

Eszter Csibra and Guy-Bart Stan

Department of Bioengineering, Imperial College Centre for Synthetic Biology (IC-CSynB),

Imperial College London, London, UK, SW7 2AY

Correspondence:
Eszter Csibra (e.csibra@imperial.ac.uk) and Guy-Bart Stan (g.stan@imperial.ac.uk)

Keywords: absolute quantification, calibration, engineering biology, fluorescent proteins, microplate reader, synthetic biology

Abbreviations: BCA, bicinchoninic acid; BSA, bovine serum albumin; EC, extinction coefficient; EDTA, ethylenediaminetetraacetic acid; FP, fluorescent protein, GFP, green fluorescent protein, MEFL, molecules of equivalent fluorescein, MEFP, molecules of equivalent fluorescent protein, OD, optical density; PEMS, particles of equivalent microspheres, SDS-PAGE, sodium dodecyl sulphate polyacrylamide gel electrophoresis; SEVA, Standardised European Vector Architecture

Abstract

This paper presents a generalisable method for the calibration of fluorescence readings on microplate readers, in order to convert arbitrary fluorescence units into absolute units. FPCountR relies on the generation of bespoke fluorescent protein (FP) calibrants, assays to determine protein concentration and activity, and a corresponding analytical workflow. We systematically characterise the assay protocols for accuracy, sensitivity and simplicity, and describe a novel 'ECmax' assay that outperforms the others and even enables accurate calibration without requiring the purification of FPs. To obtain cellular protein concentrations, we consider methods for the conversion of optical density to either cell counts or alternatively to cell volumes, as well as examining how cells can interfere with protein counting via fluorescence quenching, which we quantify and correct for the first time. Calibration across different instruments, disparate filter sets and mismatched gains is demonstrated to yield equivalent results. It also reveals that mCherry absorption at 600nm does not confound cell density measurements unless expressed to over 100,000 proteins per cell. FPCountR is presented as pair of open access tools (protocol and R package) to enable the community to use this method, and ultimately to facilitate the quantitative characterisation of synthetic microbial circuits.

41 **Introduction**

42

43 There is a growing awareness that tackling the challenge of synthetic circuit design requires
44 the synthesis of empirical characterisation data on genetic parts with mathematical
45 modelling approaches for predicting and realising desired behaviours (1–3). However, there
46 are numerous challenges in integrating experimental data with quantitative frameworks, as
47 experimental data is typically acquired in relative or arbitrary units (specific to instruments
48 and their respective settings), which cannot be converted into useful units and therefore
49 limits our ability to make comparisons between experiments and models.

50

51 Fluorescent proteins (FPs) are our most versatile tools for the assessment of synthetic
52 genetic element performance. Since their discovery, FPs have rightly been recognised as
53 uniquely valuable reporter proteins for quantitative characterisation (4,5), since they do not
54 require the addition of exogenous components to fluoresce. This makes their use easy and
55 cost effective. Various laboratory instruments allow the characterisation of fluorescent
56 systems in a wide range of dimensions and scales – through direct visualisation (using
57 fluorescence microscopy), via single-cell fluorescence analysis (using flow cytometry), or via
58 timecourse kinetic data acquisition (using microplate readers).

59

60 The 'protein quantification problem' of reporting GFP levels acquired by such instruments in
61 'relative fluorescent units' (RFU) has been widely recognised in synthetic biology (6). This
62 recognition has led to the adoption of calibration standards such as fluorescein, a small
63 molecular fluorophore with similar excitation and emission characteristics to GFP.
64 Fluorescein can be used to calibrate a given instrument by converting the instrument's

65 arbitrary RFU output into units of 'molecules of equivalent fluorescein' (MEFL). This
66 technique has been demonstrated to enable the comparison of GFP expression data
67 gathered from different instruments as well as across laboratories (6,7).
68
69 While it is now approaching mainstream usage in synthetic biology, the conversion of green
70 fluorescence values into MEFL is arguably not the most important type of quantification
71 required for building synthetic circuits. Three aspects of the protein quantification problem
72 remain elusive. First, fluorescein is only a good calibrant for green fluorescent proteins,
73 leaving blue, yellow, orange and red FPs uncalibrated. Second, fluorescein can only provide
74 a conversion to units of fluorescein, whereas what is actually needed is a conversion to units
75 of protein. Currently, most experiments cannot even reveal the order of magnitude at which
76 FPs are being expressed (ie. 10 vs 100,000 molecules per cell) – in contrast to what is
77 possible with RNA sequencing (8). Third, while fluorescein can allow the comparison of GFP
78 levels between instruments and laboratories, it cannot address the comparison between
79 two different FPs in the same circuit. This is only possible if RFUs from both FPs can be
80 separately converted into molecular units of protein. Some have attempted to tackle this by
81 attempting to predict the relative brightness of FPs using theoretical values (9,10), but such
82 calibrations make a number of assumptions, for instance about translation rate equivalence
83 across constructs, that require validation before they can be adopted.
84
85 Fortunately, there is a reasonably simple solution. The ideal calibrant in molecular biology is
86 considered to be a purified sample of the molecule to be measured – in this case, the
87 fluorescent protein itself. While purified FPs are not commercially available, they can be
88 produced 'in-house', thereby providing that crucial direct link between relative fluorescence

89 units and molecules of protein. Indeed, FP calibration has been proposed in the past,
90 though its use has been limited to microscopy (11–13) and remains rare for microplate
91 assays (14,15). We suspect this is due to (a) an underappreciation that absolute
92 quantification is possible without 'omics', (b) a reticence to try unfamiliar biochemical
93 protocols that are not usually part of the synthetic biology or microbiology repertoire, and
94 (c) doubt that such protocols could be accurate or sensitive enough for general usage. These
95 motivated us to develop a general, yet simple-to-use calibration protocol of this nature.
96
97 In what follows, we outline our optimised calibration method and present it as a pair of
98 resources: a wet lab protocol, called FPCount (available on protocols.io) and an
99 accompanying analysis package, called FPCountR (available on GitHub). We present data
100 showing the development of this protocol, and systematically characterise the biochemical
101 and analytical requirements of an accurate and sensitive calibration. We also present a
102 'hack', which acts both to simplify the method to remove the requirement for protein
103 purification, and to make it more sensitive and robust. Using FPCountR, we show that
104 conversion to molecular units can be used to calibrate across different instruments,
105 disparate filter sets and mismatched gains to yield equivalent results. We demonstrate that
106 conversion to absolute units allows the user of our method to compare the protein
107 production efficiency of different fluorescent proteins expressed from an otherwise
108 identical vector in molecules per cell, or as a molar concentration. Finally, we demonstrate
109 that this method can be used to quantitatively evaluate the experimental protocols
110 themselves, such as the extent to which red fluorescent proteins confound optical density
111 readings in timecourse assays.
112

113 **Results**

114

115 Our aim for this work was to develop a generalisable method for FP calibration that could be
116 used by any group wishing to calibrate fluorescence readings on microplate readers to
117 molecular units. To do this, we defined a number of key aims for our proposed method.
118 First, it should be accurate and sensitive, as we need the method to correctly estimate
119 molecule numbers within cells, and as protein yields from small-scale purifications are
120 typically modest. Second, the calibration protocol should be as simple as possible and
121 adapted ideally such that each respective assay may be carried out in 96-microwell plate
122 format using the same plate reader that is being calibrated. This way, multiple fluorescent
123 proteins may be calibrated at once, and end users do not require any additional
124 instrumentation. Third, the method should be suitable for the particular characteristics of
125 fluorescent proteins. These proteins are smaller and structurally distinct from typical
126 protein calibrants such as bovine serum albumin (BSA), and are known to present certain
127 challenges for quantification due to light absorption by their chromophores. Thus, any assay
128 developed for non-fluorescent proteins requires a separate validation on FPs to
129 demonstrate that they are also adequate for this class of proteins. Finally, we wanted to
130 enable the easy analysis of the data, by (i) enabling easy conversion of raw calibration data
131 into a conversion factor that links the arbitrary fluorescence output of a protein with its
132 quantity in molecular units, and (ii) allowing easy conversion of data from all future
133 timecourse data from that instrument to produce outputs in (e.g. GFP) molecules, rather
134 than relative (e.g. green) fluorescence units. An overview of the FPCount fluorescent protein
135 calibration protocol is illustrated in Fig. 1.

136

137 **Design of purification protocol for obtaining protein calibrants**

138 In order to obtain our fluorescent protein calibrants, they must first be produced by
139 overexpression, and purified. Protein purification methodologies can often be highly
140 complex, requiring specialist expertise and instrumentation. To alleviate this, our protocol
141 was explicitly designed to be as straightforward as possible, involving only the minimum
142 number of required steps, and using commonly available reagents. It was also designed to
143 be amenable to small-volume purifications to enable the calibration of multiple proteins in
144 parallel. The protocol is summarised in Fig. 2A. A standardised FP expression vector was
145 constructed from an arabinose-inducible His-tagged FP construct in a high-copy SEVA vector
146 (Fig. 2B). Overnight expression was used to maximise protein production, and cells were
147 lysed using sonication to avoid the requirement to add chemical components that may
148 interfere with downstream processes, such as EDTA (with His-tag purification) or detergents
149 (with protein quantification). Insoluble proteins were removed via centrifugation and
150 proteins were purified using cobalt resin to minimise the co-isolation of impurities.
151 Expression yields and solubility were checked by SDS-PAGE (Fig. 2C) and the quality of
152 purified FP calibrants was verified by SDS-PAGE and fluorescence excitation and emission
153 scanning (Fig. 2D-E, Supplementary Fig. 1). Purified calibrants were of consistently good
154 purity and yield.

155

156 **Conducting a plate reader calibration**

157 The calibration of plate readers with fluorescein has traditionally been conducted using a
158 dilution series of known concentrations of fluorescein, subjected to a fluorescence assay in
159 the plate reader whose calibration is desired (measurement of relative fluorescence units,
160 RFU). The results are used to relate fluorescein molecule number to RFU to obtain a

161 conversion factor, which can in turn be used to convert RFU readouts from experimental
162 data into MEFL units (6). For protein calibrants, one additional step is required: protein
163 concentration determination.
164
165 In our initial protocols, we opted for the bicinchoninic acid (BCA) assay due to its sensitivity,
166 ease of use and low protein-to-protein variability (16). In addition, microplate-optimised
167 reagents for a 'microBCA' were available from ThermoFisher, with excellent reported
168 sensitivities (to 2 ng/µl). Pilot tests showed an inhibitory effect of the Tris and NaCl in the
169 elution buffer (Supplementary Fig. 2A) suggesting that buffer exchange would be necessary
170 for high assay sensitivity. Normalised measurements using a BSA standard obtained with the
171 kit were fitted to a polynomial equation to obtain a standard curve (Supplementary Fig. 2D,
172 ii). This was then used to predict the concentrations of FPs prepared as serial dilutions by
173 first removing values under the reported threshold of sensitivity and fitting a linear model
174 through the rest of the values (Supplementary Fig. 2D, ii and iii). An extra step was added to
175 the recommended protocol (Supplementary Fig. 2A, ii and Supplementary Fig. 2C) to
176 account for baseline absorbance of red FPs in the A562 range. These calculations are
177 handled in the FPCountR package by the get_conc_bca() function. Using the resultant
178 predicted protein concentrations and fluorescence assay data on the same FP dilution
179 series, an adapted version of the generate_cfs() function from flopR (7) was used to
180 generate conversion factors (RFU/molecule) for mCherry in a Tecan Spark plate reader for
181 the red FP-typical filter set (ex 560/20, em 620/20; Supplementary Fig. 3).
182
183

184 **Development of a second assay for FP concentration – the A280 assay**

185 We sought to verify the accuracy of the BCA assay by re-quantifying our FPs with a second
186 method that is likely to give reliable concentration estimates. While a wide variety of
187 protein assays exist, the only widely-used 'absolute' assay that does not require a calibrant
188 is the A280 assay. As the name suggests, it quantifies protein concentration via light
189 absorbance at 280 nm, where three amino acid residues are known to absorb light in a way
190 that has been shown to be approximately additive (17). This means that a reasonable
191 prediction of light absorbance at 280 nm can be made for any pure protein of known
192 primary sequence by way of an extinction coefficient (EC; expected light absorption for a
193 given concentration of protein). As sample absorbance relates to molecular concentration
194 according to Beer's law, i.e., $A = EC * C * L$, (where A is the absorbance, EC is the
195 extinction coefficient ($M^{-1}cm^{-1}$), C is the concentration (M), and L is the path length (cm)),
196 the protein concentration may be calculated from absorbance using only the extinction
197 coefficient and the path length. The most common formats for A280 measurements are
198 laborious, single-throughput cuvette- or Nanodrop-type measurements, requiring the
199 adaptation of the standard A280 protocols for use in 96-well microplates. We have
200 summarised the requirements for such an adaptation in Supplementary Note 1 and
201 Supplementary Fig. 4-8. In brief, the best results for A280 assays were obtained by using UV-
202 clear plastic, removing additives, correcting for path length variation, and correcting for light
203 scatter. This required the collection of an absorbance spectrum from 200-1000 nm rather
204 than just one reading at 280 nm, and is processed by two consecutive FPCountR functions,
205 plot_absorbance_spectrum() and get_conc_a280() (Supplementary Fig. 6-7).

206

207

208 **Systematic testing of the calibration protocol allows method validation**

209 We sought to conduct a systematic assessment of the BCA and A280 methods by testing
210 three spectrally distinct FPs in two buffers, assessed with both assays in parallel (Fig. 3). The
211 chosen FPs (mTagBFP2, mGFPmut3 and mCherry) are widely used, monomeric, reasonably
212 fast-maturing and bright. All three are almost identical on the protein level to their FPbase
213 entries (Fig. 2B; Materials & Methods; Supplementary Data), with the exception that they all
214 have a His_6 tag N-terminal extension, and mGFPmut3 includes a well-defined monomeric
215 A206K mutation (18,19). The chosen buffers (T5N15 (5mM Tris-HCl pH 7.5, 15 mM NaCl)
216 and T5N15 with protease inhibitors) were both compatible with the microBCA assay
217 (Supplementary Fig. 2B), however, pilot studies suggested they might have different effects
218 on the A280 assay. Following purification, FPs were initially dialysed to remove additives,
219 then re-dialysed into the respective assay buffer (Fig. 3A). Each FP:buffer combination was
220 then serially diluted, and subjected to an absorbance scan (200-1000 nm measurement, for
221 the A280), a fluorescence assay (fluorescence measurement with appropriate filters for
222 each FP) and a microBCA assay (reagent addition, incubation and A562 measurement). The
223 results of this comparative test are shown in Fig. 3B-C, Supplementary Fig. 9 and
224 Supplementary Tables 1-2. Broadly, the results from each assay validate those of the other
225 assay: the measured concentration of each FP using the microBCA and A280 assays are
226 within 2-fold of each other for most samples (Fig. 3C) and apparent linear ranges reach 1
227 ng/µl for most dilution series (Fig. 3B). For comparison, the reported sensitivity on the
228 Nanodrop is 100 ng/µl (20). We observed some buffer sensitivity for both assays – the
229 microBCA produces more linear results in the buffer containing protease inhibitors, whereas
230 the A280 does better in the buffer without them. Buffer effects were also apparent for the
231 fluorescence assay (Supplementary Note 2, Supplementary Fig. 10). Conversion factors

232 obtained from different purification batches gave similar estimates where concentration
233 estimates were made using optimal assay:buffer pairings, varying between 1.02 and 1.63-
234 fold (Supplementary Fig. 9B).
235
236 **FPbase-enabled ECmax method performs better than conventional assays**
237 We trialled a third protein assay during this experiment, designated here as the 'ECmax'
238 method. The principal idea behind this assay is that the A280 extinction coefficient is not
239 the only known extinction coefficient for FPs. FPs also possess an extinction coefficient ('EC')
240 corresponding to their light absorption at their peak ('max') excitation wavelength. As the
241 'ECmax' of most FPs is available on FPbase, we can automate its retrieval using the FPbase
242 API (21). The analytical processing steps for the ECmax assay (in get_conc_ecmax()) are
243 similar to those of the A280 assay (Supplementary Fig. 8), and require no further readings.
244 As the maximal absorbance peaks for all FPs tested were higher than those at 280 nm
245 (Supplementary Fig. 1B, Supplementary Table 3), we anticipated that the ECmax assay
246 would be more sensitive. Further, as protease inhibitors absorb at wavelengths under 300
247 nm, we hypothesised this assay may be less buffer-sensitive. Compellingly, both appear to
248 be true: we consistently found that the ECmax assay produced larger linear ranges and
249 lower limits of detection than the other assays (approaching 0.1 ng/µl, 10-fold better than
250 the A280 assay and 1000-fold better than a Nanodrop), and that it produced almost
251 indistinguishable results whether or not the buffer contained protease inhibitors (Fig. 3B-C,
252 Supplementary Fig. 9, Supplementary Table 1). In addition, predictions from the ECmax
253 assay closely match those from the A280, typically predicting concentrations matching at
254 80-100 % those of the expected result (rather than 170-220% for microBCA; Fig. 3C,
255 Supplementary Table 3). For these reasons, we propose that the ECmax assay would be the

256 most robust assay to include in a simple calibration protocol and will proceed using
257 concentrations calculated from ECmax assays in what follows.
258
259 **ECmax assay enables FP calibration without protein purification**
260 Having established that the ECmax assay, a protein quantification assay that relies only on
261 the peak light absorbance of each FP, is highly accurate and sensitive for purified proteins
262 measured using trusted methods, we asked whether this method could enable us to drop
263 the purification step altogether. Dropping the purification step was not possible for the
264 other assays as they are designed to quantify total protein concentrations, but the ECmax
265 should in principle be specific for the considered FP and may therefore be used to quantify
266 FPs in crude lysates. To investigate this, we harvested and lysed cells expressing our three
267 FPs, separated the soluble fractions and concentrated them. Putting these through an
268 ECmax assay and fluorescence assay, we observed it was possible to quantify FPs in crude
269 lysates with high sensitivity (to 1 ng/µl), and to obtain almost identical conversion factor
270 values as from our purified FPs (Fig. 3E-F). Of two lysis methods tested – sonication and
271 chemical lysis – the former produced more accurate results. It can therefore be
272 demonstrated that by establishing the ECmax assay for FP quantification, it is possible to
273 remove the purification step altogether without compromising calibration accuracy.
274
275 **Calibration allows comparison across instruments for FPs other than GFP**
276 While fluorescein enables the comparison of experimental results across laboratories and
277 instruments by converting arbitrary units into 'molecules of equivalent fluorescein' (MEFL)
278 units, FP calibration in principle offers the same capability by converting arbitrary units into
279 units of 'molecules of equivalent FP' (MEFP), which is carried out using FPCountR's

280 process_plate() function (Fig. 4A-B). This allows us to quantify the number of FP molecules
281 in each well of our microplates. To calculate uncalibrated 'per cell' values, typical studies
282 will divide the RFU values by the optical density (OD600 or OD700) of the culture, which
283 quantifies cell density. The calibration of optical density to particle number can be achieved
284 through a similar calibration process using microspheres of similar size to *E. coli* (22,23).
285 Using both calibrations, it is possible to quantify molecule number per cell in 'molecules of
286 equivalent FP per particles of equivalent microspheres' (MEFP/PEMS, Fig. 4C), units which
287 should allow cross comparison between different instruments, gains and filter sets. To test
288 this, overnight cultures of *E. coli* containing mCherry expression vectors were split into
289 separate but identical microplates containing arabinose, and were grown in two plate
290 readers using a range of settings. The results show that normalised values of relative
291 fluorescence differ by ~1.5, ~3 and ~130-fold without calibration, whereas such values
292 become reliably comparable after calibration, even for experiments conducted using
293 instrument settings that produce values that cannot be legibly plotted on the same axis (Fig.
294 4D).
295
296 **Calibration allows estimation of absolute cellular protein concentration**
297 We next asked if calibration to units of MEFP/PEMS was a reasonable approximation for
298 molecule number per cell (Fig. 5A). We carried out microsphere calibration using 1 cm
299 cuvettes and a standard spectrophotometer and obtained conversion factors
300 (Supplementary Table 4) that fell within the range quantified by empirical OD600-specific
301 cell counts (24). In addition, other authors have confirmed that values of fluorescent protein
302 per cell using fluorescein and microsphere calibrants (MEFL/PEMS) are approximately equal
303 to those obtained using fluorescein-calibrated single cell data on a flow cytometer (7,23),

304 suggesting particle counts were likely to approximate actual cell numbers. However, we
305 observed a major caveat to the use of microspheres as calibrants, which is that their
306 absorbance profiles differ from that of cells. This can frustrate their ability to provide
307 accurate conversions between 'per cell' data calculated using OD700 versus OD600
308 measurements (Supplementary Fig. 11 and Supplementary Tables 4-5) for which we discuss
309 solutions in Supplementary Note 3.
310
311 The question of whether the measured fluorescence of FPs in cells is the equivalent of
312 measured fluorescence of the same number of FPs *in vitro* is less clear. Some authors have
313 found that cells attenuate (or 'quench') fluorescence (15,25), but the magnitude of the
314 effect has not been systematically investigated, particularly for modest cell concentrations
315 found in a typical *E. coli* growth assay. We quantified the quenching properties of *E. coli* cells
316 on our three FPs by mixing an increasing concentration of non-fluorescent cells with purified
317 FPs, and quantifying the difference in apparent fluorescence with added cells (Fig. 5B and
318 Supplementary Fig. 12). Our results suggest that this 'quenching' effect amounts to less than
319 20 % of the fluorescence signal for moderate cell densities (OD600/cm under 0.5), but
320 increases to ~30 % for the highest cell densities typically observed in microplate-scale
321 cultures (OD600/cm around 2). This information was used to add a correction step into the
322 process_plate() calculations so as to compensate for the expected percentage loss of
323 fluorescence with increasing cell density (Fig. 5B, right panel). The complete analytical
324 workflow from calibration to experimental data processing is illustrated in Supplementary
325 Fig. 13.
326

327 Using these amendments, it is possible to convert response curve assay data into molecules
328 per cell. Figure 5C shows one experiment using mCherry expression construct in two vectors
329 with different origins of replication. Using these vectors, we obtain figures for mCherry
330 abundance that vary between about 3,000 to 80,000 molecules per cell for p15A, and 1,000
331 to 600,000 for colE1. Protein abundance information, available from proteomics and
332 ribosome profiling studies, suggests that the typical *E. coli* protein is present in the order of
333 10^2-10^3 copies per cell, and the most abundant are present in the order of 10^5 copies per
334 cell or higher (26–28). Over-induction using the high-copy (colE1) vector therefore appears
335 to allow synthetic protein expression to reach the level of the most abundant proteins in the
336 cell. This is supported by the fact that these vectors reliably overexpress FPs to a level
337 observable by SDS-PAGE in unpurified lysates (Fig. 1, Supplementary Fig. 1). Modest
338 expression (10^2-10^3 per cell) can be achieved by combining low arabinose concentrations
339 with either vector. Leaky expression could be quantified in the colE1 vector as contributing
340 hundreds of mCherry molecules per cell even without induction, whereas in the p15A vector
341 it was merely ten copies per cell. In other words, the colE1 vector allows us to utilise the full
342 spectrum of protein abundances from modestly expressed enzymes such as the RecBCD
343 helicase (~100 copies per cell) through to the most abundant ribosomal proteins (~100,000
344 copies per cell, (28)). We could also use this to compare the number of molecules produced
345 from the same vectors but two different FPs. Interestingly, measurements from identical
346 SEVA vectors revealed that while the FP abundances were in the same order of magnitude,
347 mTagBFP2 accumulated to higher levels per cell than mCherry by 1.83-fold on average,
348 despite sharing the same promoter, 5' untranslated region, ribosome binding site and N-
349 terminal protein sequences (Fig. 5C-D).
350

351 In 2011, Volkmer and colleagues noted that while OD-specific *E. coli* cell counts varied with
352 growth rate, the OD-specific total cell volume was approximately 3.6 µl per OD600/cm,
353 regardless of strain or growth condition (24). Using OD as a measure of the cumulative
354 cellular volume in a culture could therefore be used to convert fluorescence and OD
355 measurements into concentrations in molar units, instead of 'per cell' values, and such
356 conversions may be more appropriate for comparing experimental results with quantitative
357 modelling of cellular reaction networks, since they are unaffected by growth rate
358 differences. Using this method, we found that FP abundances using the same vectors
359 populate a range of concentrations between 0.01-100 µM (Fig. 5D).
360
361 **Absolute quantification reveals hidden properties of fluorescent proteins**
362 Finally, we were interested in testing whether absolute quantification could illuminate a
363 well-known source of error in bacterial assays. The presence of red FPs has been suggested
364 to interfere with bacterial cell density estimations at 600 nm since red FPs typically absorb
365 well at this wavelength (29) and has led to the conclusion that circuits using red FPs must be
366 quantified at 700 nm, which is unaffected by their presence. However, the number of
367 molecules of red FPs that might be required for this effect to occur has never been
368 quantified.
369
370 Calibrated timecourse data of mCherry overexpression in *E. coli* (Fig. 6) was examined to
371 quantify these effects, with mGFPmut3 and mTagBFP2 used as negative controls. The ratio
372 between OD600 and OD700 measurements was used to identify errors caused by red FP
373 absorbance. Linear models fitted to the relationship between measured OD600 and OD700
374 values confirmed that this relationship was very similar for all uninduced cells (Fig. 6B;

375 OD600 = 1.30 * OD700 – 0.02), but mCherry induction resulted in a measurable deviation
376 (OD600 = 1.37 * OD700 – 0.03, Fig. 6B-C). Looking at the relationship between this shift and
377 cellular protein copy number (Fig. 6D), our results indicated that the OD600 error for
378 mCherry was only apparent when mCherry levels per cell were high (over 100,000 per cell),
379 and that the magnitude of this error was only about 5 %. In contrast, mGFPmut3 expression
380 had no effect on cell density estimation using OD600, as expected. Surprisingly, we
381 observed the opposite trend for mTagBFP2, in which OD600 measurement appeared to
382 underestimate cell density where mTagBFP2 was expressed at high levels per cell. The
383 reasons for this are currently unclear and beyond the scope of this paper, but our results
384 suggest that this could be an interesting avenue for future work. Generally, this experiment
385 confirmed that the presence of low to moderate FP levels per cell (under 100,000) do not
386 perturb cell density estimates, and errors are of a lower magnitude in all cases than those
387 from cellular fluorescence quenching.
388
389 **Discussion**
390
391 Our aim for this work was to develop a generalisable method that allows fluorescence
392 readings on microplate readers to be calibrated to molecular units of fluorescent protein.
393 The method ought to be (1) accurate and sensitive, (2) as simple as possible, (3) suitable for
394 any fluorescent protein, and (4) easily analysed. To develop the method, we adopted the
395 principles of redundant experimental design, including the validation of multiple assay
396 types, characterisation of the method's consistency, and the assessment of its generality for
397 three different FPs (30).
398

399 Our initial method using a simple purification protocol (Fig. 2) and a commercial protein
400 assay allowed us to develop an analysis pipeline to obtain conversion factors from purified
401 FP calibrants. To demonstrate the accuracy and validity of our calibrations, we verified that
402 the absorbance and fluorescence spectra of the calibrants matched their counterparts on
403 FPbase (Fig. 1, Supplementary Fig. 2; (21,31)), and validated our initial protein assay
404 measurements by cross comparison with two further methods. To do this, we adapted the
405 low-throughput A280 assay into an accurate, high-throughput assay format, and showed
406 that these were suitable for use with FPs even though some absorb in the near-UV range.
407 This type of assay for FP quantification has not, to our knowledge, been demonstrated in
408 the literature before, and we contend that it is likely to be of particular interest since it
409 requires no calibrant or commercial reagent, no expensive quartz-based consumables and
410 exhibits a sensitivity that exceeds that of commercial systems such as the Nanodrop.
411
412 We also discovered a methodological 'hack' to obtaining FP concentrations using the
413 extinction coefficients at their maximum excitation wavelength, the ECmax assay, which was
414 both the simplest and the most robust of all the assays tested. Specifically, the ECmax assay
415 was the least affected by buffer conditions, and had the largest linear range (to almost 0.1
416 ng/µl; Fig. 3). We note that the assay is limited by the fact that it requires the used FP to be
417 documented on FPbase, and assumes that the documented ECmax measured by other
418 laboratories is accurate. Promisingly, our results suggest good inter-lab agreement for these
419 measurements (compare A280 and ECmax estimates, Fig. 3C). In addition, an analysis of all
420 FPs on FPbase, comparing the proteins' extinction coefficients at 280 nm versus at their
421 maximum excitation wavelength, supports the idea that the ECmax is a more sensitive assay
422 for most FPs (Supplementary Fig. 14, Supplementary Table 3). While the EC(280) values are

423 highly uniform (median: 27,400 $M^{-1}cm^{-1}$), likely because most FPs are very similar in size, the
424 ECmax values are mostly considerably larger (median: 64,200 $M^{-1}cm^{-1}$). Impressively, as the
425 ECmax assay specifically quantifies FP concentration rather than total protein concentration,
426 we were also able to show that it is possible to do these calibrations in crude lysate without
427 compromising on accuracy, demonstrating that calibrants may be produced without affinity
428 purification (Fig. 3D-F). Overall, we expect calibrations carried out using the ECmax method,
429 using either purified calibrants or (sonicated) cell lysates, to be equally accurate. We provide
430 both rigorous and expedient protocols for prospective users on protocols.io.
431
432 Such calibrations can then be used, first, to enable the comparison of experimental results
433 from different plate readers or across different settings, in molecules of fluorescent protein
434 per particles of equivalent microspheres (MEFP/PEMS; Fig. 4B). This is akin to using
435 fluorescein but with a broader application range, since using bespoke calibrants for each FP
436 allows us to calibrate instruments for any FP regardless of its spectral characteristics. If used
437 merely as comparative units, the precision (repeatability) of each calibration is important,
438 but their accuracy (whether conversions predict molecule numbers as closely as possible) is
439 not. Second, they can be used to express protein abundance as 'molecules per cell' (Fig. 5C).
440 Accuracy here is an important consideration, and will not only depend on the accuracy of
441 the FP calibration (discussed above), but also on the microsphere calibration, and the
442 removal of any interactions between absorbance and fluorescence characteristics of cells
443 expressing FPs. As to microsphere calibration, cross-comparison with flow cytometry data
444 suggests cell count estimates from microsphere calibrations are reasonable (7,23), although
445 Beal and colleagues used 0.961 µm microspheres whose size is closer to *E. coli* than those
446 used in this study (0.890 µm; the larger type are now unavailable). Our protein abundance

447 estimates (10^2-10^5 proteins per cell; Fig. 5B) are also within reasonable bounds (26,28),
448 corroborating their use, and indicating that FP calibrations may enable protein abundance
449 comparisons between microplate assays and proteomics experiments.
450
451 The consideration of whether the presence of cells interferes with fluorescence
452 quantification (or vice versa) is multifaceted. It is well known that cells interfere with
453 fluorescence measurements through autofluorescence. Cellular autofluorescence is known
454 to largely impact GFP quantification accuracy (32), and is corrected for in FPCountR by
455 normalising to the background fluorescence of control cells at a similar OD (akin to (7,15)).
456 The 'quenching' of apparent FP fluorescence by the presence of cells is more rarely
457 considered (14,15). We have found that the effect size is comparable for different FPs
458 (Supplementary Fig. 12), unlike for autofluorescence, supporting previous observations by
459 others (25). A correction for this attenuation in FPCountR compensates fluorescence
460 according to the expected percentage quenched at the measured OD (Fig. 5B). Both of these
461 corrections are included in the process_plate() function.
462
463 Overall, it seems likely that the accuracy of calibrated molecule counts per cell may be
464 limited by the accuracy of cell count calibration, since it is known that OD-specific cell
465 counts change with growth rate, and that this is due to the positive relationship between
466 growth rate and cell size for *E. coli* (24). We therefore expect these calculations of protein
467 counts per cell will be more accurate where cell size and microsphere size are as similar as
468 possible, and inaccuracies will arise if the differences become significant. Thus, these values
469 are likely to be approximately accurate so long as the following assumptions are true: that *E.*
470 *coli* absorbance (scatter) is well represented by microsphere properties, and that it doesn't

471 change significantly over time or between samples. These will likely to be true for many *E.*
472 *coli* experiments since cell shrinkage has been shown to take place only after several hours
473 in stationary culture, and only large growth rate differences maintained for prolonged
474 periods were observed to make a significant difference to cell size in exponentially growing
475 cells (24), but may fail if circuits impose significant burden on host cell resources that
476 impacts growth rate or cell size (33–35). In contrast, using a conversion from OD to total cell
477 volume in a given culture well allows us to remove the requirement for counting cells (Fig.
478 5D) and allows the expression of protein concentrations as 0.01-100 µM. These figures
479 should be approximately accurate under the assumption that the OD-specific cell volume
480 doesn't vary significantly between samples or over time. This is strongly supported by the
481 results of Volkmer and colleagues (24) whose data suggests this variation is within 2-fold
482 across a wide range of growth conditions, but also by others who have shown that as cell
483 volumes increase, their OD-specific cell counts decrease by approximately the same
484 magnitude (33,36). Units of concentration may also be more meaningful for reaction
485 modelling since ultimately it is molecular concentration that is critical for binding and
486 kinetics (9,37,38).
487
488 We used absolute protein quantification to investigate the problem first described by Hecht
489 and colleagues (29) in which an association between mCherry overexpression and
490 deviations in cell density measurements were made. Repeating these assays showed a clear
491 effect, but this effect was of modest magnitude (<5%) and was only apparent at very high
492 mCherry levels per cell (over 10^5 molecules per cell; Fig. 6). This suggests that for most
493 circuits that use moderate expression levels to minimise cellular burden, OD600 values
494 would remain an accurate way to quantify cell density. We also unexpectedly observed the

495 opposite effect in mTagBFP2 expressions. As this analysis was technically a quantification of
496 whether OD600 and OD700 measurements deviate from each other in the presence of
497 different FPs, these results might not suggest that OD600-based cell density readings in the
498 presence of high mTagBFP2 are inaccurate. It might instead suggest that, conversely for
499 mTagBFP2, the OD700 readings are inaccurate. We do not currently have an explanation for
500 this finding. One possible contributing factor may be that while it is often described as one
501 of the best blue FPs, mTagBFP2 has a higher propensity to aggregate than mCherry and
502 most GFPs (39). Cell stress is known to induce *E. coli* to elongate (33,40), which may affect
503 its scattering properties. It is possible that very high FP levels may frequently cause a small
504 but significant error in cell density estimates due to combinations of effects from light
505 absorption and scatter that warrants more study in order to allow us to further improve
506 molecular quantifications of FPs under those conditions.
507
508 While flow cytometry and mass spectrometry allow us to probe single-cell measurements or
509 the protein complement of an entire cell, respectively, microplate readers remain an
510 important screening platform in the Design-Build-Test-Learn cycle due to ease of use, low
511 cost and high iterative capabilities. This necessitates the development of methods for
512 extracting informative numbers from such data. The ability to extract absolute protein
513 abundance information from assays of engineered microbial cells is imperative to enable
514 the characterisation, optimisation and tuning of genetic circuits in a rigorous and
515 quantitative manner, and will allow for a deeper insight into how protein abundance affects
516 genetic construct behaviour, cellular burden and growth rate. Importantly, our approach
517 enables accurate, non-destructive, and easy protein abundance comparisons, even between
518 samples that differ in growth rate or cell size.

519

520 Further, such absolute quantification need not be limited to fluorescent proteins. The last
521 few years have seen a fantastic expansion of fluorogenic molecules, tools that have allowed
522 the specific quantification of localised proteins (41–43), proteins in anaerobic environments
523 (44,45), and the fluorescent quantification of RNAs (38,46,47). Calibration of these
524 molecules would be more complex to achieve but no less valuable. Equally, calibration of
525 alternative instruments such as flow cytometers are also of interest, but would require a
526 very different approach, requiring calibrants to be attached to particles of cell-like sizes. We
527 hope that our demonstration of how to achieve absolute FP quantifications from microplate
528 reader assays using FPCountR can contribute to the effort to develop more quantitative
529 approaches for the analysis of circuit behaviour in synthetic biology and beyond.

530

531 **Materials and Methods**

532

533 **Materials**

534 Primers and gblocks were obtained from IDT, and *E. coli* strain DH5-alpha (Invitrogen,
535 18265-017) was used for molecular cloning. Chemicals and protein reagents were purchased
536 from Merck, Sigma, ThermoFisher Scientific, and Bio-Rad, molecular biology reagents from
537 NEB and Life Technologies and general laboratory reagents from Corning, Greiner Bio-One,
538 Starlab and VWR.

539

540 **Fluorescent proteins**

541 The mCherry (48) protein sequence was based on the FPbase entry for mcherry (FPbase ID:
542 ZERB6) with the following changes: M1(MVHHHHHHGSG). The mGFPmut3 (49) protein

543 sequence was based on the FPbase entry for gfpmut3 (FPbase ID: A20WC) with the
544 following changes: M1(MVHHHHHHGSG), A206K (a substitution to make the protein
545 monomeric; (18,19)). The mTagBFP2 (50) protein sequence was based on the FPbase entry
546 for mtagbfp2 (FPbase ID: ZO7NN) with the following changes: M1(MVHHHHHHGSG). Full
547 protein sequences are provided in Supplementary Table 6.
548
549 **DNA assembly**
550 Vectors for fluorescent protein purification and growth curve assays were constructed
551 according to standard protocols, via Golden Gate and Gibson assembly techniques using *E.*
552 *coli* strain DH5α (Invitrogen, 18265-017). Constructs were assembled into Standardised
553 European Vector Architecture (SEVA) backbones (51): pS381 was generated from pS181
554 with chloramphenicol substitution; pS361 was generated similarly from pS161. In an effort
555 to approximately equalise expression levels between different proteins, the 5' untranslated
556 region (including ribosome binding site) and 5' region of each construct was set to be
557 identical up to residue 11 (coding region begins: *DNA*:
558 ATGGTTCACCATCATCATCACcacGGTtcgggc, *protein*: MVHHHHHHGSG). The second residue
559 was set to valine to reduce the effects of N-end mediated degradation (52). The affinity tag
560 chosen for purification was the His_6 tag, which was followed by a short unstructured linker
561 (GSG). Full DNA sequences of vectors are provided in Supplementary Table 6.
562
563 **FPCount (wet lab) protocol**
564 The protocols are available on protocols.io. In total, we have described three FPCount
565 calibration protocols: (1) the full protocol using FP purification and three protein assays for
566 cross-validation, as conducted in Fig. 3 available at https://www.protocols.io/view/fpcount-

567 protocol-full-protocol-bztsp6ne (53), (2) a short protocol requiring purification but using the
568 ECmax assay only, available at https://www.protocols.io/view/fpcount-protocol-short-
569 protocol-bzt6p6re (54), and (3) the purification-free protocol that uses FPs in lysates for
570 calibration, available at https://www.protocols.io/view/fpcount-protocol-in-lysate-
571 purification-free-proto-bzudp6s6 (55). It is anticipated that users will have differing
572 requirements concerning protocol time and validation, so we have provided all three
573 protocols.
574
575 **Protein expression and harvesting**
576 Fluorescent proteins were produced using pS381 (SEVA) expression vectors in *E. coli*
577 BL21(DE3) strains. Glycerol stocks were inoculated into 50 ml Luria Broth (Miller)
578 supplemented with 50 µg/ml chloramphenicol and 0.02 % arabinose and were grown
579 overnight at 30 °C at 250 rpm. Cells were harvested after ~16 h by transferring them to
580 prechilled containers on ice. All further steps were conducted on ice. OD600 readings were
581 taken, and 40 OD of cells was transferred to fresh falcon tubes, washed once in T50N300 (50
582 mM Tris-HCl pH 7.5, 300 mM NaCl) and resuspended in lysis buffer (T50N300, 1X protease
583 inhibitors (EDTA-free, Pierce A32955), filter sterilised, supplemented with lysozyme 100
584 µg/µl). Cells were separated into 20 OD (2 ml) fractions and sonicated (Qsonica Q125
585 sonicator, 50% amplitude, 10s on, 10s off, 2 min). Lysates were supplemented with 5 mM
586 $CaCl_2$, 50 mM $MgCl_2$ and treated with DNase I (50 U/ml, bovine pancreas, MP Biomedicals,
587 219006210) for 30 min at 4 °C. Soluble fractions were isolated by isolation of the
588 supernatant after centrifugation (16,000 xg, 30 min, 4 °C), and both fractions were checked
589 by SDS-PAGE followed by staining with Coomassie-based dye according to the
590 manufacturer's instructions (Instant Blue Protein Stain, Sigma ISB1L-1L).

591

592 **Protein purification**

593 Fluorescent proteins were purified in batch using His-tag affinity chromatography at room
594 temperature according to the resin manufacturer's instructions (Thermo Fisher). Lysates
595 were supplemented with 10 mM imidazole and 600 µl was applied to HisPur Cobalt resin
596 (300 µl, ThermoFisher) equilibrated in Binding Buffer (T50N300+pi, 10 mM imidazole),
597 mixed and incubated at room temperature for ~15 min before removal (1,000 xg, 1 min).
598 This was repeated four times, before the resin was washed with 10 column volumes of
599 Binding Buffer. Protein was eluted in Elution Buffer (T50N300+pi, 150 mM imidazole). All
600 protein fractions for calibration were stored protected from light at 4 ^{o}C.

601

602 **Preparation for calibration assays**

603 Elution fractions were combined and concentrated approximately 10-fold using Amicon
604 centrifugal filter columns (Merck, UFC5010), followed by buffer exchange (1000x) into
605 T5N15 (5mM Tris-HCl pH 7.5, 15 mM NaCl) or T5N15+pi (T5N15, 1x protease inhibitors, filter
606 sterilised).

607

608 **Microplate reader assays.** All assays were carried out using a Tecan Spark microplate reader
609 except the fluorescence spectra assays, which were carried out using a BMG Clariostar Plus
610 microplate reader.

611

612 **Calibration assays.** For each FP calibration, both concentration and fluorescence assays
613 were carried out on the same dilution series of protein. Concentrated, buffer exchanged FP
614 (100 µl) was diluted in 900 µl buffer, then diluted 1:2 into 500 µl buffer in 1.5 ml

615 eppendorfs. A total of 11 dilutions were prepared in this way, distributed into UV-
616 transparent microplates (Greiner, 655801) as duplicates (225 µl). Bovine serum albumin
617 (BSA) standards (from Micro BCA Protein Assay kit, ThermoFisher, 23235) were prepared in
618 parallel with the same buffer(s). This dilution set was then subjected to the protein
619 concentration and fluorescence assays.
620
621 **Protein concentration assays: A280 assay and ECmax assay**
622 Absorbance assays were carried out on 225 µl protein in UV-transparent plates, using the
623 Spark absorbance scan method (see Supplementary Methods).
624
625 **Fluorescence assays**
626 Following absorbance scans, 200 µl from each well of the original plate was transferred into
627 clear polystyrene plates (Corning, 3370). This plate was sealed (Eppendorf Masterclear real-
628 time PCR film adhesive, 30132947) and used to run the Spark fluorescence methods (see
629 Supplementary Methods) on all relevant instruments, channels and gains.
630
631 **Protein concentration assays: microBCA assay**
632 BCA assays were carried out using the Micro BCA Protein Assay kit (ThermoFisher, 23235)
633 according to the manufacturer's instructions (microplate protocol). Briefly, 150 µl of
634 working reagent was dispensed into a clean microplate, and 150 µl from each well of the
635 fluorescence assay plate was mixed into the reagent with a multichannel pipettor. Reactions
636 were covered with a plate seal (BreatheEasy sealing membrane, Sigma, Z380059), and
637 subjected to the Spark microBCA method (see Supplementary Methods).
638

639 **Calibration of OD600 and OD700 values using microspheres**

640 Calibration of optical density readings used to quantify cell number (OD600 and OD700) was
641 carried out according to published protocols (7). The microspheres used were monodisperse
642 silica microspheres (Cospheric, SiO2MS-2.0, 2.0g/cc, d50=0.890um, CV=3.2%, <1% Doubles).

643

644 **Bacterial timecourse assays**

645 DH10B *E. coli* transformants were grown overnight in M9 medium (M9 salts (1X, Sigma
646 M6030), casamino acids (0.2%), fructose (0.8%), thiamine HCl (0.25 mg/ml), $MgSO_4$ (2 mM),
647 $CaCl_2$ (0.1 mM)) supplemented with 50 µg/ml chloramphenicol, in a deep-well plate (30 °C,
648 700 rpm), and diluted the following morning into fresh M9 with antibiotic (deep-well plate,
649 30 °C, 700 rpm) to an OD600 (cm^{-1}) of 0.05. After 1 hour, cultures were transferred into
650 clear 96-well microplates (Corning, 3370) with pre-loaded arabinose (5 µl). Plates were
651 sealed (BreatheEasy sealing membrane, Sigma, Z380059) and grown in a Tecan Spark plate
652 reader in kinetic mode (see Supplementary Methods, Spark growth curve method).

653

654 **Analytical methods**

655 All data was analysed using R (56). The FPCountR package that was developed for the FP
656 calibrations is available on GitHub at https://github.com/ec363/fpcountr (57). For a
657 summary of the functions, see the Fig. 1 and Supplementary Fig. 13.

658

659 **Fluorescence scans**

660 Excitation and emission spectra of the fluorescent proteins were conducted using a BMG
661 Clariostar Plus microplate reader in sealed plates (Corning, 3370; Eppendorf Masterclear

662 real-time PCR film adhesive, 30132947) at wavelengths appropriate to each FP (see
663 Supplementary Methods).
664
665 **Figures**
666 Figures were created using RStudio and Biorender.com.
667
668 **Data availability**
669 Computer code produced in this study is available on the following repositories:
670 - R package for data analysis: GitHub (https://github.com/ec363/fpcountr)
671 This study includes no data deposited in external repositories.
672
673 **Acknowledgements**
674 GBS and EC acknowledge funding from the Royal Academy of Engineering (RAEng CiET
675 1819\5).
676
677 **Author contributions**
678 EC and GBS conceived the study. EC conducted the experiments, analysed the data and
679 wrote the R package. EC and GBS wrote the manuscript.
680
681 **Conflict of Interest**
682 The authors declare no conflict of interest.
683
684 **References**
685 1. Delvigne F, Zacchetti B, Fickers P, Fifani B, Roulling F, Lefebvre C, et al. Improving control
686 in microbial cell factories: from single cell to large-scale bioproduction. FEMS Microbiol

687 Lett [Internet]. 2018 Sep 24 [cited 2021 Nov 26]; Available from:
688 https://academic.oup.com/femsle/advance-
689 article/doi/10.1093/femsle/fny236/5106341

690 2. Beal J, Goñi-Moreno A, Myers C, Hecht A, Vicente M del C, Parco M, et al. The long
691 journey towards standards for engineering biosystems: Are the Molecular Biology and
692 the Biotech communities ready to standardise? EMBO Rep [Internet]. 2020 May 6
693 [cited 2021 Nov 26];21(5). Available from:
694 https://onlinelibrary.wiley.com/doi/10.15252/embr.202050521

695 3. Perrino G, Hadjimitsis A, Ledesma-Amaro R, Stan G-B. Control engineering and synthetic
696 biology: working in synergy for the analysis and control of microbial systems. Curr Opin
697 Microbiol [Internet]. 2021 Aug 1 [cited 2021 Jun 3];62:68–75. Available from:
698 https://www.sciencedirect.com/science/article/pii/S1369527421000655

699 4. Chalfie M, Tu Y, Euskirchen G, Ward WW, Prasher DC. Green fluorescent protein as a
700 marker for gene expression. Science [Internet]. 1994 Feb 11 [cited 2021 Jan
701 18];263(5148):802–5. Available from:
702 https://science.sciencemag.org/content/263/5148/802

703 5. Rodriguez EA, Campbell RE, Lin JY, Lin MZ, Miyawaki A, Palmer AE, et al. The Growing
704 and Glowing Toolbox of Fluorescent and Photoactive Proteins. Trends Biochem Sci.
705 2017 Feb;42(2):111–29.

706 6. Beal J, Haddock-Angelli T, Baldwin G, Gershater M, Dwijayanti A, Storch M, et al.
707 Quantification of bacterial fluorescence using independent calibrants. PLOS ONE
708 [Internet]. 2018 Jun 21 [cited 2020 Jun 29];13(6):e0199432. Available from:
709 https://journals.plos.org/plosone/article?id=10.1371/journal.pone.0199432

710 7. Fedorec AJH, Robinson CM, Wen KY, Barnes CP. FlopR: An Open Source Software
711 Package for Calibration and Normalization of Plate Reader and Flow Cytometry Data.
712 ACS Synth Biol [Internet]. 2020 Sep 18 [cited 2021 Nov 26];9(9):2258–66. Available
713 from: https://pubs.acs.org/doi/10.1021/acssynbio.0c00296

714 8. Gorochowski TE, Chelysheva I, Eriksen M, Nair P, Pedersen S, Ignatova Z. Absolute
715 quantification of translational regulation and burden using combined sequencing
716 approaches. Mol Syst Biol. 2019 03;15(5):e8719.

717 9. Boada Y, Vignoni A, Alarcon-Ruiz I, Andreu-Vilarroig C, Monfort-Llorens R, Requena A, et
718 al. Characterization of Gene Circuit Parts Based on Multiobjective Optimization by
719 Using Standard Calibrated Measurements. ChemBioChem [Internet]. 2019 Oct 15
720 [cited 2021 Nov 26];20(20):2653–65. Available from:
721 https://onlinelibrary.wiley.com/doi/10.1002/cbic.201900272

722 10. Vignoni A, Boada Y, Boada Acosta L, Andreu-Vilarroig C, Alarcón I, Requena A, et al.
723 Fluorescence calibration and color equivalence for quantitative synthetic biology. IFAC-
724 Pap [Internet]. 2019 [cited 2021 Nov 26];52(26):129–34. Available from:
725 https://linkinghub.elsevier.com/retrieve/pii/S2405896319321305

11. Taniguchi Y, Choi PJ, Li G-W, Chen H, Babu M, Hearn J, et al. Quantifying E. coli Proteome and Transcriptome with Single-Molecule Sensitivity in Single Cells. 2010;329:8.

12. Finan K, Raulf A, Heilemann M. A Set of Homo-Oligomeric Standards Allows Accurate Protein Counting. Angew Chem Int Ed [Internet]. 2015 Oct 5 [cited 2021 Nov 26];54(41):12049–52. Available from: https://onlinelibrary.wiley.com/doi/10.1002/anie.201505664

13. Tie HC, Madugula V, Lu L. The development of a single molecule fluorescence standard and its application in estimating the stoichiometry of the nuclear pore complex. Biochem Biophys Res Commun [Internet]. 2016 Sep [cited 2021 Nov 26];478(4):1694–9. Available from: https://linkinghub.elsevier.com/retrieve/pii/S0006291X16314486

14. Canton B, Labno A, Endy D. Refinement and standardization of synthetic biological parts and devices. Nat Biotechnol [Internet]. 2008 Jul [cited 2022 Jan 3];26(7):787–93. Available from: https://www.nature.com/articles/nbt1413

15. Hirst CD, Ainsworth C, Baldwin G, Kitney RI, Freemont PS. Protocol for the Standardisation of Transcriptional Measurements. In: McGenity TJ, Timmis KN, Nogales B, editors. Hydrocarbon and Lipid Microbiology Protocols [Internet]. Berlin, Heidelberg: Springer Berlin Heidelberg; 2015 [cited 2021 Nov 26]. p. 9–26. (Springer Protocols Handbooks). Available from: http://link.springer.com/10.1007/8623_2015_148

16. Noble JE, Knight AE, Reason AJ, Di Matola A, Bailey MJA. A Comparison of Protein Quantitation Assays for Biopharmaceutical Applications. Mol Biotechnol [Internet]. 2007 Sep 13 [cited 2021 Nov 26];37(2):99–111. Available from: http://link.springer.com/10.1007/s12033-007-0038-9

17. Pace CN, Vajdos F, Fee L, Grimsley G, Gray T. How to measure and predict the molar absorption coefficient of a protein. Protein Sci [Internet]. 1995 Nov [cited 2021 Nov 26];4(11):2411–23. Available from: https://onlinelibrary.wiley.com/doi/10.1002/pro.5560041120

18. Zacharias DA, Violin JD, Newton AC, Tsien RY. Partitioning of Lipid-Modified Monomeric GFPs into Membrane Microdomains of Live Cells. Science [Internet]. 2002 May 3 [cited 2021 Nov 26];296(5569):913–6. Available from: https://www.science.org/doi/10.1126/science.1068539

19. Shaner NC, Steinbach PA, Tsien RY. A guide to choosing fluorescent proteins. Nat Methods [Internet]. 2005 Dec [cited 2021 Nov 26];2(12):905–9. Available from: https://www.nature.com/articles/nmeth819

20. Thermo Fisher Scientific. NanoDrop 1000 Spectrophotometer, V3.8 User's Manual [Internet]. 2010 [cited 2021 Nov 26]. Available from: https://tools.thermofisher.com/content/sfs/manuals/nd-1000-v3.8-users-manual-8%205x11.pdf

764 21. Lambert TJ. FPbase: a community-editable fluorescent protein database. Nat Methods
765 [Internet]. 2019 Apr [cited 2021 Nov 26];16(4):277–8. Available from:
766 http://www.nature.com/articles/s41592-019-0352-8

767 22. Stevenson K, McVey AF, Clark IBN, Swain PS, Pilizota T. General calibration of microbial
768 growth in microplate readers. Sci Rep [Internet]. 2016 Dec [cited 2021 Nov
769 26];6(1):38828. Available from: http://www.nature.com/articles/srep38828

770 23. Beal J, Farny NG, Haddock-Angelli T, Selvarajah V, Baldwin GS, Buckley-Taylor R, et al.
771 Robust estimation of bacterial cell count from optical density. Commun Biol [Internet].
772 2020 Dec [cited 2021 Nov 26];3(1):512. Available from:
773 https://www.nature.com/articles/s42003-020-01127-5

774 24. Volkmer B, Heinemann M. Condition-Dependent Cell Volume and Concentration of
775 Escherichia coli to Facilitate Data Conversion for Systems Biology Modeling. Langowski
776 J, editor. PLoS ONE [Internet]. 2011 Jul 29 [cited 2021 Nov 26];6(7):e23126. Available
777 from: https://dx.plos.org/10.1371/journal.pone.0023126

778 25. Zhang C, Liu M-S, Han B, Xing X-H. Correcting for the inner filter effect in measurements
779 of fluorescent proteins in high-cell-density cultures. Anal Biochem. 2009 Jul
780 15;390(2):197–202.

781 26. Ishihama Y, Schmidt T, Rappsilber J, Mann M, Hartl FU, Kerner MJ, et al. Protein
782 abundance profiling of the Escherichia coli cytosol. BMC Genomics [Internet]. 2008
783 [cited 2021 Nov 26];9(1):102. Available from:
784 http://bmcgenomics.biomedcentral.com/articles/10.1186/1471-2164-9-102

785 27. Arike L, Valgepea K, Peil L, Nahku R, Adamberg K, Vilu R. Comparison and applications of
786 label-free absolute proteome quantification methods on Escherichia coli. J Proteomics
787 [Internet]. 2012 Sep [cited 2021 Nov 26];75(17):5437–48. Available from:
788 https://linkinghub.elsevier.com/retrieve/pii/S1874391912004861

789 28. Li G-W, Burkhardt D, Gross C, Weissman JS. Quantifying Absolute Protein Synthesis
790 Rates Reveals Principles Underlying Allocation of Cellular Resources. Cell [Internet].
791 2014 Apr [cited 2021 Nov 26];157(3):624–35. Available from:
792 https://linkinghub.elsevier.com/retrieve/pii/S0092867414002323

793 29. Hecht A, Endy D, Salit M, Munson MS. When Wavelengths Collide: Bias in Cell
794 Abundance Measurements Due to Expressed Fluorescent Proteins. ACS Synth Biol
795 [Internet]. 2016 Sep 16 [cited 2019 Dec 10];5(9):1024–7. Available from:
796 https://doi.org/10.1021/acssynbio.6b00072

797 30. Casadevall A, Fang FC. Rigorous Science: a How-To Guide. mBio [Internet]. 2016 Dec 30
798 [cited 2021 Nov 3];7(6). Available from:
799 https://journals.asm.org/doi/10.1128/mBio.01902-16

800 31. Raynal B, Lenormand P, Baron B, Hoos S, England P. Quality assessment and
801 optimization of purified protein samples: why and how? Microb Cell Factories

802 [Internet]. 2014 Dec [cited 2021 Nov 26];13(1):180. Available from:
803 http://microbialcellfactories.biomedcentral.com/articles/10.1186/s12934-014-0180-6

804 32. Lichten CA, White R, Clark IB, Swain PS. Unmixing of fluorescence spectra to resolve
805 quantitative time-series measurements of gene expression in plate readers. BMC
806 Biotechnol [Internet]. 2014 Dec [cited 2021 Nov 26];14(1):11. Available from:
807 https://bmcbiotechnol.biomedcentral.com/articles/10.1186/1472-6750-14-11

808 33. Basan M, Zhu M, Dai X, Warren M, Sévin D, Wang Y, et al. Inflating bacterial cells by
809 increased protein synthesis. Mol Syst Biol [Internet]. 2015 Oct [cited 2021 Nov
810 26];11(10):836. Available from:
811 https://onlinelibrary.wiley.com/doi/10.15252/msb.20156178

812 34. Ceroni F, Algar R, Stan G-B, Ellis T. Quantifying cellular capacity identifies gene
813 expression designs with reduced burden. Nat Methods [Internet]. 2015 May [cited
814 2019 Mar 14];12(5):415–8. Available from:
815 http://www.nature.com/articles/nmeth.3339

816 35. Boo A, Ellis T, Stan G-B. Host-aware synthetic biology. Curr Opin Syst Biol [Internet].
817 2019 Apr [cited 2020 Jun 26];14:66–72. Available from:
818 https://linkinghub.elsevier.com/retrieve/pii/S245231001930006X

819 36. Schaechter M, MaalØe O, Kjeldgaard NOY 1958. Dependency on Medium and
820 Temperature of Cell Size and Chemical Composition during Balanced Growth of
821 Salmonella typhimurium. Microbiology [Internet]. 1958 [cited 2021 Nov 26];19(3):592–
822 606. Available from:
823 https://www.microbiologyresearch.org/content/journal/micro/10.1099/00221287-19-
824 3-592

825 37. Bloom RJ, Winkler SM, Smolke CD. A quantitative framework for the forward design of
826 synthetic miRNA circuits. Nat Methods [Internet]. 2014 Nov [cited 2021 Nov
827 26];11(11):1147–53. Available from: http://www.nature.com/articles/nmeth.3100

828 38. Siegal-Gaskins D, Tuza ZA, Kim J, Noireaux V, Murray RM. Gene Circuit Performance
829 Characterization and Resource Usage in a Cell-Free “Breadboard”. ACS Synth Biol
830 [Internet]. 2014 Jun 20 [cited 2021 Nov 26];3(6):416–25. Available from:
831 https://pubs.acs.org/doi/10.1021/sb400203p

832 39. Cranfill PJ, Sell BR, Baird MA, Allen JR, Lavagnino Z, de Gruiter HM, et al. Quantitative
833 assessment of fluorescent proteins. Nat Methods [Internet]. 2016 Jul [cited 2020 Jul
834 3];13(7):557–62. Available from: http://www.nature.com/articles/nmeth.3891

835 40. Justice SS, Hunstad DA, Cegelski L, Hultgren SJ. Morphological plasticity as a bacterial
836 survival strategy. Nat Rev Microbiol [Internet]. 2008 Feb [cited 2021 Nov 26];6(2):162–
837 8. Available from: http://www.nature.com/articles/nrmicro1820

838 41. Svendsen S, Zimprich C, McDougall MG, Klaubert DH, Los GV. Spatial separation and
839 bidirectional trafficking of proteins using a multi-functional reporter. BMC Cell Biol

840 [Internet]. 2008 Dec [cited 2021 Nov 26];9(1):17. Available from:
841 https://bmcmolcellbiol.biomedcentral.com/articles/10.1186/1471-2121-9-17

842 42. Li C, Mourton A, Plamont M-A, Rodrigues V, Aujard I, Volovitch M, et al. Fluorogenic
843 Probing of Membrane Protein Trafficking. Bioconjug Chem [Internet]. 2018 Jun 20
844 [cited 2019 Mar 20];29(6):1823–8. Available from:
845 http://pubs.acs.org/doi/10.1021/acs.bioconjchem.8b00180

846 43. Csibra E, Renders M, Pinheiro V. Bacterial cell display as a robust and versatile platform
847 for the engineering of low affinity ligands and enzymes. ChemBioChem [Internet]. 2020
848 May 15 [cited 2020 May 26];cbic.202000203. Available from:
849 https://onlinelibrary.wiley.com/doi/abs/10.1002/cbic.202000203

850 44. Streett HE, Kalis KM, Papoutsakis ET. A Strongly Fluorescing Anaerobic Reporter and
851 Protein-Tagging System for *Clostridium* Organisms Based on the Fluorescence-
852 Activating and Absorption-Shifting Tag Protein (FAST). Kivisaar M, editor. Appl Environ
853 Microbiol [Internet]. 2019 Jul 15 [cited 2021 Nov 26];85(14). Available from:
854 https://journals.asm.org/doi/10.1128/AEM.00622-19

855 45. Charubin K, Streett H, Papoutsakis ET. Development of Strong Anaerobic Fluorescent
856 Reporters for Clostridium acetobutylicum and Clostridium ljungdahlii Using HaloTag
857 and SNAP-tag Proteins. Kelly RM, editor. Appl Environ Microbiol [Internet]. 2020 Oct
858 [cited 2021 Nov 26];86(20). Available from:
859 https://journals.asm.org/doi/10.1128/AEM.01271-20

860 46. Pothoulakis G, Ceroni F, Reeve B, Ellis T. The Spinach RNA Aptamer as a Characterization
861 Tool for Synthetic Biology. ACS Synth Biol [Internet]. 2014 Mar 21 [cited 2021 Nov
862 26];3(3):182–7. Available from: https://pubs.acs.org/doi/10.1021/sb400089c

863 47. Yerramilli VS, Kim KH. Labeling RNAs in Live Cells Using Malachite Green Aptamer
864 Scaffolds as Fluorescent Probes. ACS Synth Biol [Internet]. 2018 Mar 16 [cited 2021
865 Nov 26];7(3):758–66. Available from:
866 https://pubs.acs.org/doi/10.1021/acssynbio.7b00237

867 48. Shaner NC, Campbell RE, Steinbach PA, Giepmans BNG, Palmer AE, Tsien RY. Improved
868 monomeric red, orange and yellow fluorescent proteins derived from Discosoma sp.
869 red fluorescent protein. Nat Biotechnol [Internet]. 2004 Dec [cited 2020 May
870 22];22(12):1567–72. Available from: https://www.nature.com/articles/nbt1037

871 49. Cormack BP, Valdivia RH, Falkow S. FACS-optimized mutants of the green fluorescent
872 protein (GFP). Gene [Internet]. 1996 Jan [cited 2019 Oct 23];173(1):33–8. Available
873 from: https://linkinghub.elsevier.com/retrieve/pii/0378111995006850

874 50. Subach OM, Cranfill PJ, Davidson MW, Verkhusha VV. An Enhanced Monomeric Blue
875 Fluorescent Protein with the High Chemical Stability of the Chromophore. PLOS ONE
876 [Internet]. 2011 Dec 8 [cited 2021 Jan 13];6(12):e28674. Available from:
877 https://journals.plos.org/plosone/article?id=10.1371/journal.pone.0028674

878 51. Silva-Rocha R, Martínez-García E, Calles B, Chavarría M, Arce-Rodríguez A, de las Heras
879 A, et al. The Standard European Vector Architecture (SEVA): a coherent platform for
880 the analysis and deployment of complex prokaryotic phenotypes. Nucleic Acids Res
881 [Internet]. 2013 Jan [cited 2021 Nov 26];41(Database issue):D666–75. Available from:
882 https://www.ncbi.nlm.nih.gov/pmc/articles/PMC3531073/

883 52. Mogk A, Schmidt R, Bukau B. The N-end rule pathway for regulated proteolysis:
884 prokaryotic and eukaryotic strategies. Trends Cell Biol [Internet]. 2007 Apr 1 [cited
885 2021 Nov 26];17(4):165–72. Available from: https://www.cell.com/trends/cell-
886 biology/abstract/S0962-8924(07)00028-1

887 53. Csibra E, Stan G-B. FPCount protocol - Full protocol. protocols.io [Internet]. 2021 [cited
888 2021 Dec 5]; Available from: https://www.protocols.io/view/fpcount-protocol-full-
889 protocol-bztsp6ne

890 54. Csibra E, Stan G-B. FPCount protocol - Short protocol. protocols.io [Internet]. 2021 [cited
891 2021 Dec 5]; Available from: https://www.protocols.io/view/fpcount-protocol-short-
892 protocol-bzt6p6re

893 55. Csibra E, Stan G-B. FPCount protocol - in-lysate (purification free) protocol. protocols.io
894 [Internet]. 2021 [cited 2021 Dec 5]; Available from:
895 https://www.protocols.io/view/fpcount-protocol-in-lysate-purification-free-proto-
896 bzudp6s6

897 56. R Core Team. R: The R Project for Statistical Computing [Internet]. 2021 [cited 2021 Dec
898 5]. Available from: https://www.r-project.org/

899 57. Csibra E. FPCountR: Fluorescent protein calibration for plate readers [Internet]. Zenodo;
900 2021 [cited 2021 Dec 5]. Available from: https://zenodo.org/record/5760028

901

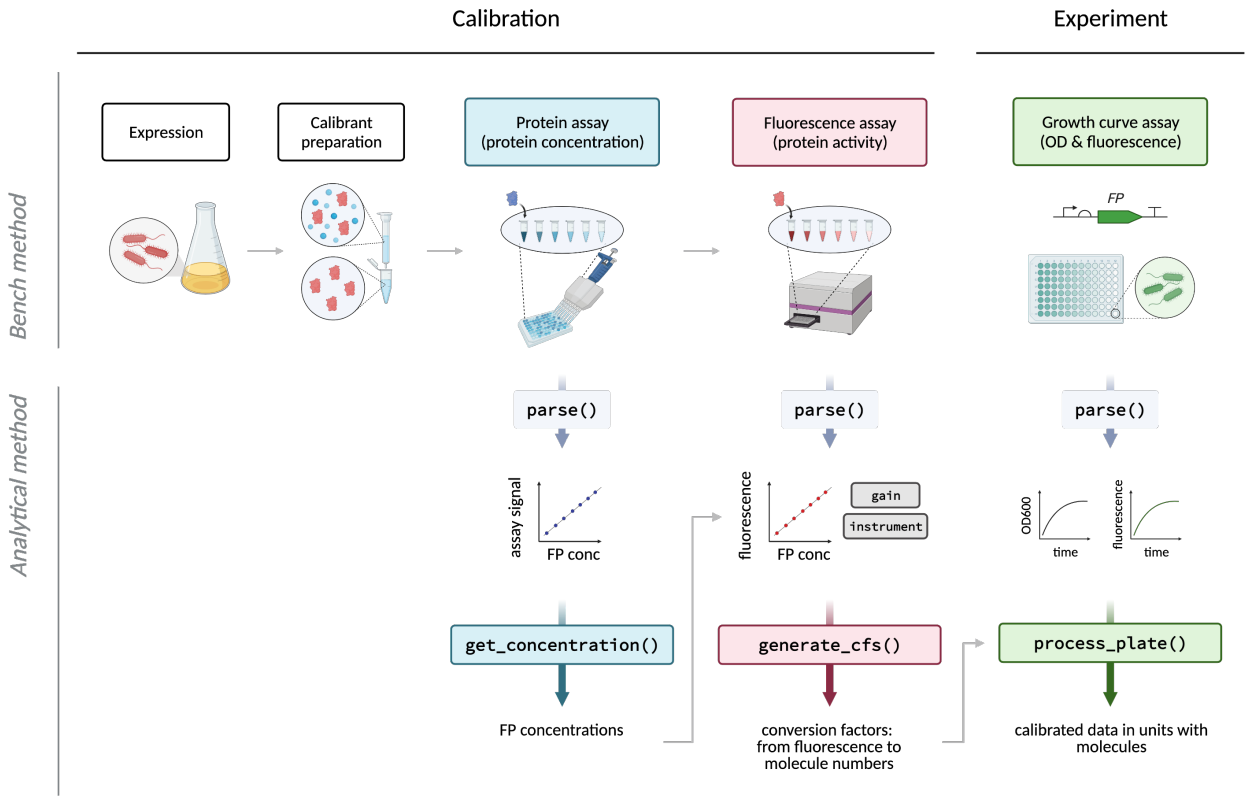

Figure 1. Overview of fluorescent protein calibration workflow using FPCountR. A calibration workflow is described *(left)*, followed by a demonstration of how this calibration can be used to convert experimental data from arbitrary fluorescence units per optical density into molecules per cell *(right)*. The calibration workflow consists of a wet lab protocol (*top, available on protocols.io*) and an analysis package (*bottom, available on GitHub*). In brief, the protocol describes how to prepare fluorescent protein calibrants by expression and purification, though the latter step is optional as lysates allow accurate calibration without the need for purification. The protocol also describes how to collect data for the calibration for both the protein assay to determine protein concentration, as well as the fluorescence assay to determine protein activity. The analytical workflow is provided as an open source R package, complete with functions that enable the extraction of protein concentrations from protein assay data, conversion factors (arbitrary fluorescence units per molecule) from a combination of protein and fluorescence assay data, and functions that allow users to convert experimental data into absolute units.

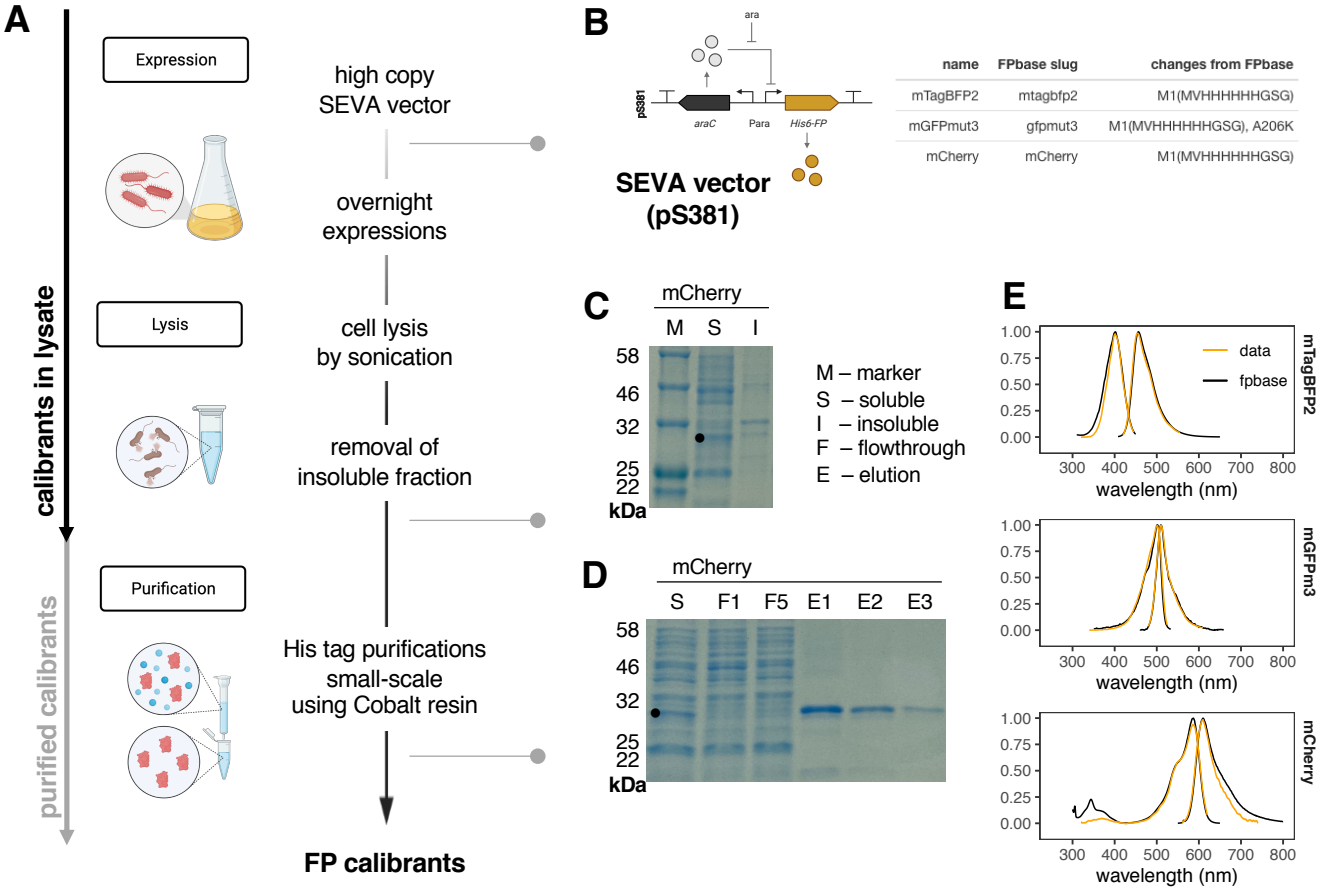
A
calibrants in lysate
purified calibrants
Expression
high copy
SEVA vector
overnight
expressions
Lysis
cell lysis
by sonication
removal of
insoluble fraction
Purification
His tag purifications
small-scale
using Cobalt resin
FP calibrants
B
ara
pS381
araC
Para
His6-FP
SEVA vector
(pS381)
name
FPbase slug
changes from FPbase
mTagBFP2
mtagbfp2
M1(MVHHHHHHGSG)
mGFPmut3
gfpmut3
M1(MVHHHHHHGSG), A206K
mCherry
mCherry
M1(MVHHHHHHGSG)
C
mCherry
M S I
58
46
32
25
22
kDa
M – marker
S – soluble
I – insoluble
F – flowthrough
E – elution
D
mCherry
S F1 F5 E1 E2 E3
58
46
32
25
22
kDa
E
data
fpbase
mTagBFP2
mGFPm3
mCherry
1.00
0.75
0.50
0.25
0.00
300 400 500 600 700 800
wavelength (nm)

Figure 2. Preparation of fluorescent protein calibrants.
A. Protocol summary. The use of high-copy vectors and overnight expression was designed to maximise protein production, and the temperature was dropped to 30 °C to minimise misfolding. Cells were lysed using sonication, to avoid the requirement to add chemical components that may interfere with downstream processes, such as EDTA (with His-tag purification) or detergents (with protein quantification), or with unknown components of 'black box' commercial lysis reagents. Insoluble proteins were removed via centrifugation and SDS-PAGE was used to confirm that the majority of the expressed FP was in the soluble fraction. Proteins were purified using His-tag affinity purification. His tags are popular affinity tags that are known for their reliability and are small in size, making them unlikely to compromise fusion protein function. Cobalt resin was used as it has higher specifity than nickel resins and is expected to co-isolate fewer impurities. The arrows on the left represent the steps required to prepare purified calibrants (grey) vs. calibrants in lysate (black). **B. Vector and FP design.** A standardised FP expression vector was constructed from an arabinose-inducible His-tagged FP construct in a high-copy SEVA vector. Three commonly-used FPs from across the spectral range were chosen for testing this protocol: mTagBFP2, mGFPmut3, and mCherry. A table of the three proteins illustrates any changes in protein sequence compared to their FPbase counterparts, showing identical matches with the exception of affinity tags and a monomerising mutation for GFPmut3. **C. Expression and solubility verification.** SDS-PAGE analysis of lysates after separation of the insoluble fraction was used to make sure that most of the fluorescent protein was soluble. The displayed SDS-PAGE is from an mCherry purification, showing the separation of the soluble (S) vs. insoluble (I) fraction, next to the protein marker (M) on a 12 % gel. **D. Purification verification.** SDS-PAGE analysis after purification was used to confirm the success of purifications. The displayed SDS-PAGE is from an mCherry purification, showing the separation of the soluble (S) fraction, next to two flowthrough (F) fractions from the binding steps showing efficient FP binding to the cobalt resin, and three elution (E) fractions. **E. Fluorescence spectra.** Fluorescence spectral scans were used to confirm that the purified FP behaves as expected. The figure shows obtained spectra (normalised such that the highest value = 1) fitted to a loess model with a 95% confidence interval (orange) overlaid with FPbase spectra (black) for each FP. Displayed spectra represent one sample measured in duplicate, that is representative of at least 2 independently purified batches of calibrant.

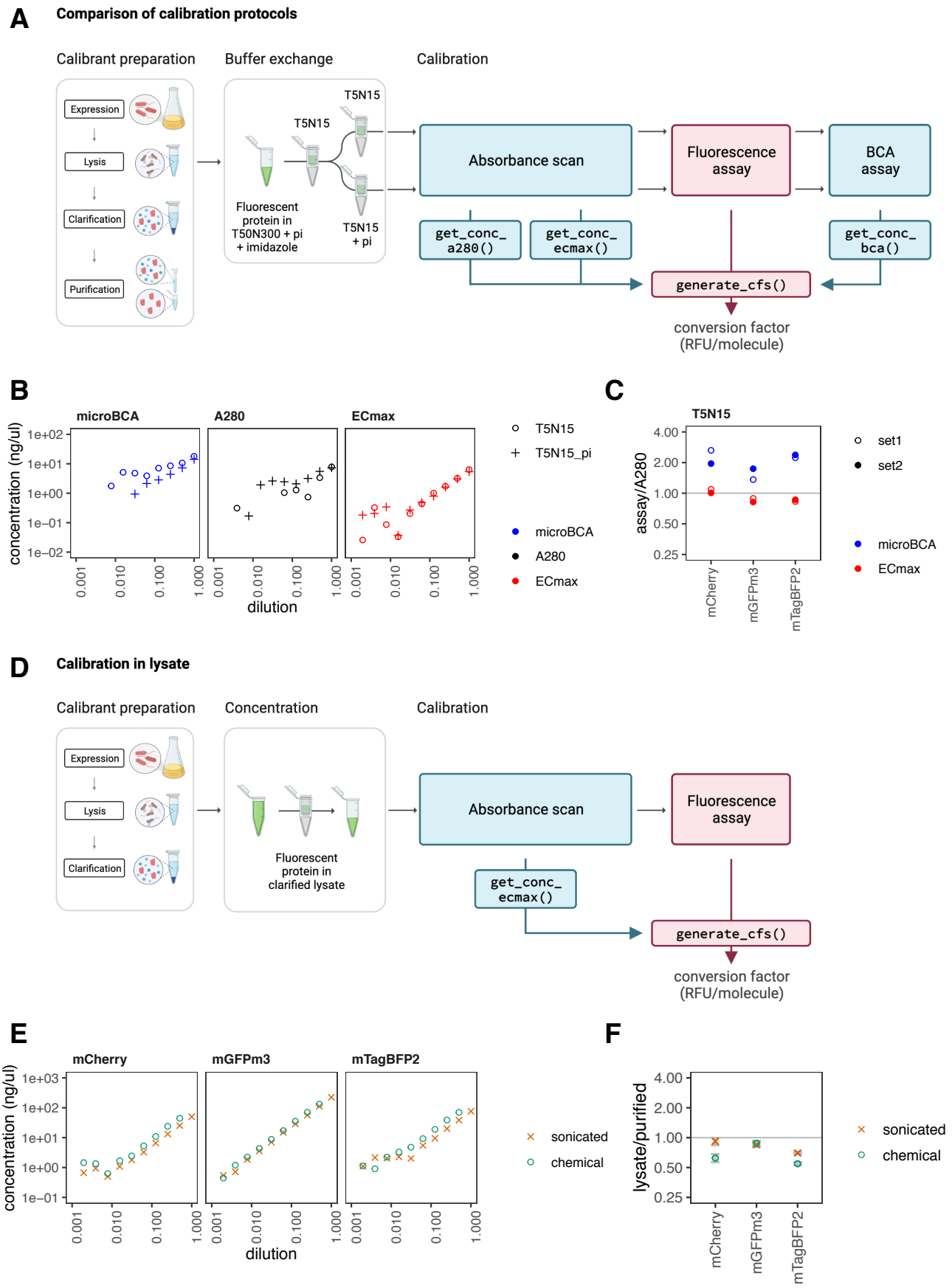
A
Comparison of calibration protocols
Calibrant preparation
Buffer exchange
Calibration
Expression
Lysis
Clarification
Purification
T5N15
T5N15
Fluorescent protein in T50N300 + pi + imidazole
T5N15 + pi
Absorbance scan
Fluorescence assay
BCA assay
get_conc_a280()
get_conc_ecmax()
get_conc_bca()
generate_cfs()
conversion factor (RFU/molecule)
B
microBCA
A280
ECmax
concentration (ng/ul)
1e+02
1e+01
1e+00
1e−01
1e−02
0.001
0.010
0.100
1.000
dilution
T5N15
T5N15_pi
microBCA
A280
ECmax
C
T5N15
assay/A280
4.00
2.00
1.00
0.50
0.25
mCherry
mGFPm3
mTagBFP2
set1
set2
microBCA
ECmax
D
Calibration in lysate
Calibrant preparation
Concentration
Calibration
Expression
Lysis
Clarification
Fluorescent protein in clarified lysate
Absorbance scan
Fluorescence assay
get_conc_ecmax()
generate_cfs()
conversion factor (RFU/molecule)
E
mCherry
mGFPm3
mTagBFP2
concentration (ng/ul)
1e+03
1e+02
1e+01
1e+00
1e−01
0.001
0.010
0.100
1.000
dilution
sonicated
chemical
F
lysate/purified
4.00
2.00
1.00
0.50
0.25
mCherry
mGFPm3
mTagBFP2
sonicated
chemical

Figure 3. Systematic characterisation of calibration protocols reveals novel assay that allows calibration in crude lysates.

A-C. Characterisation of calibration methods using purified proteins. A. Sample preparation and assay workflow. Purified FPs in elution buffer (T50N300 with protease inhibitors (pi) and imidazole) were dialysed (1) into T5N15 and then again (2) into T5N15 or T5N15 with pi. Serial dilutions of each of these FPs in both buffers were then prepared, and each dilution was subjected to three protein assays (microBCA, A280 and ECmax assay) as well as the fluorescence assay. **B. Effect of buffer and assay on measured protein concentration of each dilution.** An example of how the buffer and choice of assay effect the measured protein concentrations using a dilution series of mTagBFP2 protein (for full results see Supplementary Fig. 9). The serial dilution was a 2-fold dilution, where 11 dilutions were prepared and measured in duplicate. Points represent the mean of the duplicate values. All dilutions were measured with the A280 and ECmax assays but only the top 8 dilutions were tested with the microBCA assay. The values for the A280 and ECmax assays were normalised for scatter as indicated in Supplementary Table 2. Any missing data points had concentrations recorded as being below 0.01 ng/μl. **C. Effect of assay on calculated protein concentration compared to the A280.** The raw data of each serial dilution, as displayed in B, was fitted to a linear model and used to estimate the concentration of the first sample in the series (where the dilution factor = 1), according to methods for each assay as set out in Supplementary Fig. 2, 7 and 8. For a given FP batch (set), the microBCA and ECmax assay error was calculated by taking the fold difference in concentration predicted by the named assay, versus that predicted by the A280 assay using T5N15 buffer. Each point therefore represents one value for each FP batch. The full data for this figure can be found in Supplementary Table 1.

D-F. FP calibration in crude lysates. D. Sample preparation and assay workflow. Calibration in lysate requires fewer steps: affinity purification is omitted, buffer exchange is not required (optionally, lysates may be concentrated to increase signal), and dilution series are subject to only two assays requiring no commercial reagents or incubation steps. **E. Measured protein concentrations of FPs in lysate with ECmax assay.** Dilution series using lysates obtained by sonication (orange) or chemical lysis using the commercial B-PER reagent (Thermo Fisher, green), were measured with an absorbance scan and get_conc_ecmax(). Data plotted as in B. The top dilution of each series using chemical lysis was removed due to excessive sample scatter. **F. Difference between conversion factors using lysate vs purified protein.** Conversion factors were compared by calculating the fold difference (lysate/purified protein) at each gain. Plots display mean fold differences across the gains and error bars represent the standard deviations.

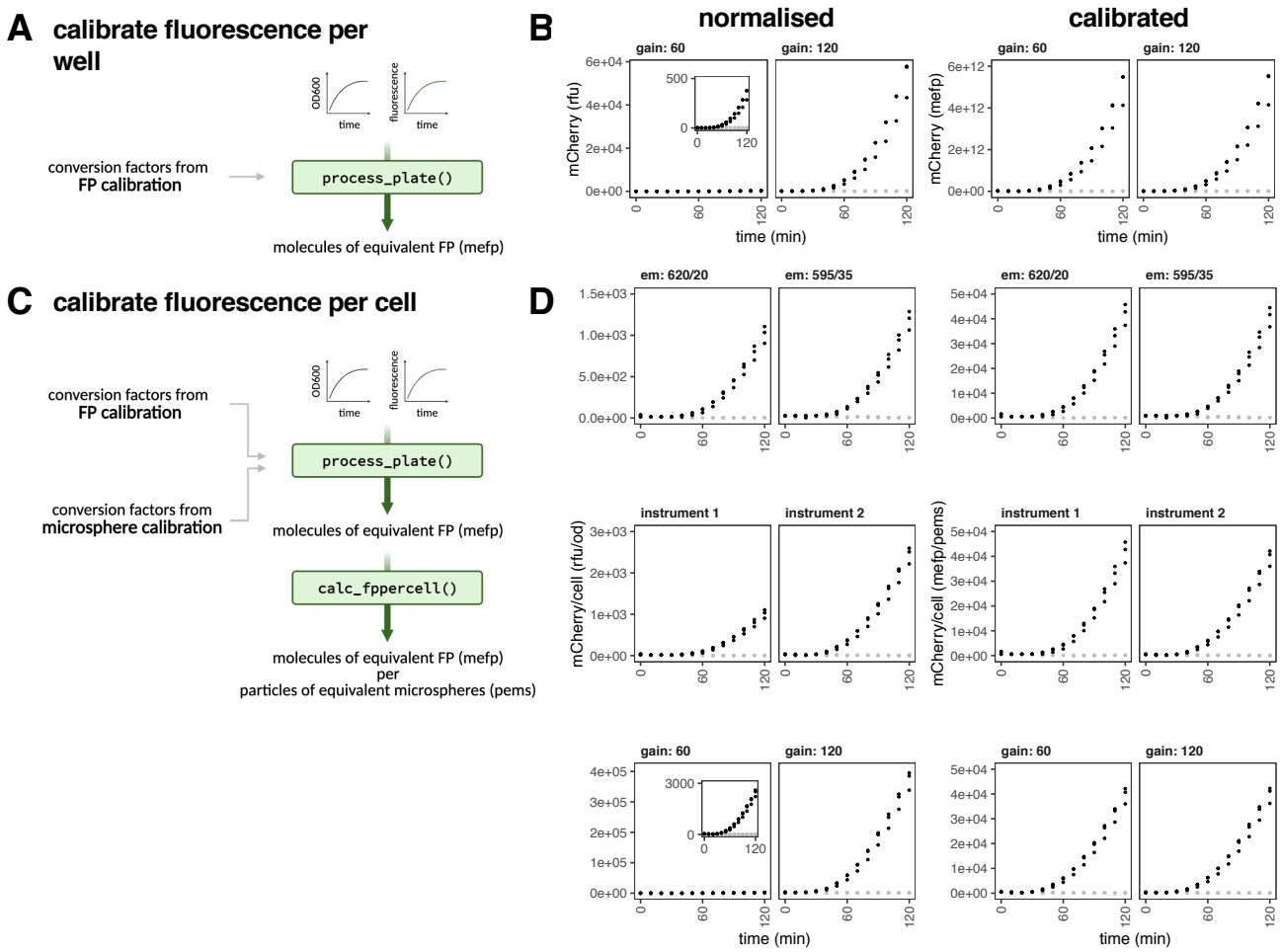

Figure 4. FP calibration allows comparison across gains and instruments for FPs other than GFP. **A. Calibration of fluorescence per well in units of MEFP.** Timecourse experimental data of *E. coli* protein expression may be processed using the process_plate() function using conversion factors obtained from FP calibration. This allows the conversion of normalised data (in relative fluorescence units, rfu) to be converted into calibrated units, of 'molecules of equivalent fluorescent protein' or 'MEFP'. **B. Comparison of normalised vs calibrated data in MEFP.** Starter cultures of *E. coli* DH10B containing pS381_ara_mCherry were transferred into a 96-well plate. mCherry expression was uninduced (grey) or induced 0.1% (black) arabinose at 0 minutes. Absorbance at OD700 and fluorescence was monitored every ten minutes. Data was collected from three biological replicates, each of which is plotted. *Left panel*: normalised mCherry in units of RFU. *Right panel*: calibrated mCherry in units of MEFP. Inset plot shows the same data as the parent plot on a zoomed axis. **C. Calibration of fluorescence per cell in units of MEFP/PEMS.** By combining the FP conversion factors with conversion factors from a microsphere calibration the data can be further processed using the calc_fppercell() function into 'per cell' data with units of MEFP per 'particles of equivalent microspheres'' (PEMS). **D. Comparison of normalised vs calibrated data in MEFP/PEMS.** Expressions were carried out as in B. Normalised and calibrated values are shown when compared across different filter sets (*top,* notation: emission wavelength/bandwidth), instruments (*middle*) and gains (*bottom*). Data for the filter and gain comparisons were taken using the same instrument.

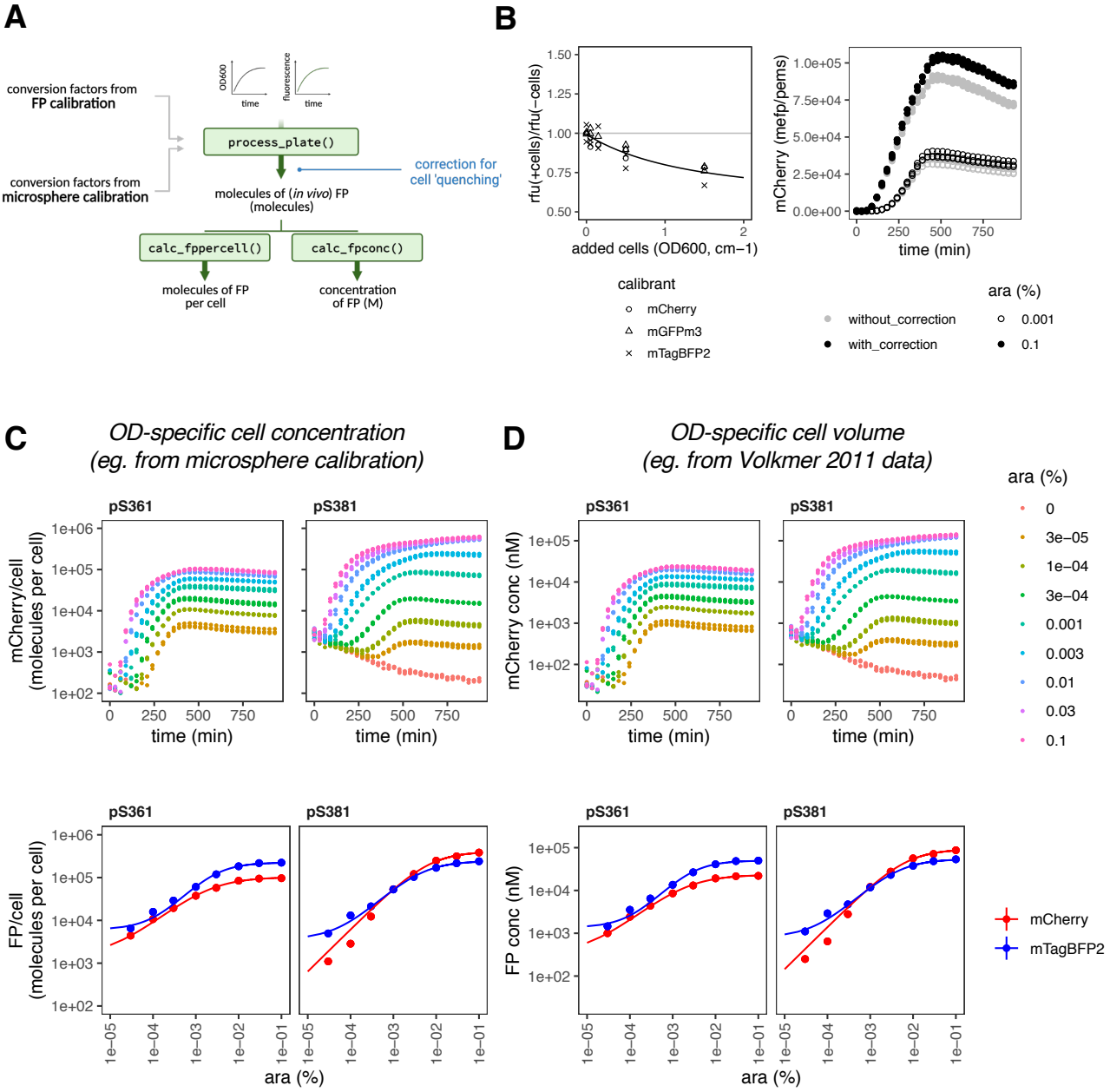
A
conversion factors from
FP calibration
conversion factors from
microsphere calibration
OD600
time
fluorescence
time
process_plate()
correction for
cell 'quenching'
molecules of (in vivo) FP
(molecules)
calc_fppercell()
calc_fpconc()
molecules of FP
per cell
concentration
of FP (M)
B
rfu(+cells)/rfu(−cells)
added cells (OD600, cm−1)
mCherry (mefp/pems)
time (min)
calibrant
mCherry
mGFPm3
mTagBFP2
without_correction
with_correction
ara (%)
0.001
0.1
C
OD-specific cell concentration
(eg. from microsphere calibration)
pS361
pS381
mCherry/cell
(molecules per cell)
time (min)
FP/cell
(molecules per cell)
ara (%)
D
OD-specific cell volume
(eg. from Volkmer 2011 data)
mCherry conc (nM)
FP conc (nM)
ara (%)
0
3e−05
1e−04
3e−04
0.001
0.003
0.01
0.03
0.1
mCherry
mTagBFP2

Figure 5. Absolute quantification of *E. coli* timeseries data in molecules per cell.
A. Functions to convert experimental data to absolute units. Diagram of modifications to the process_plate() function to (i) incorporate a compensation step based on a quantitative understanding of the impact of cell density on apparent fluorescence (this allows the units to be recorded as molecules per cell), and (ii) to calculate molecular concentration of each FP instead, in molar units. **B. Quantification of the quenching effect on fluorescence on three FPs.** Purified FPs were mixed with non-fluorescent *E. coli* at a range of concentrations, and OD600 and fluorescence intensity were recorded. After normalising for cellular autofluorescence, the fold differences between relative fluorescence intensity (rfu) with (+) and without (-) added cells was quantified *(left)*. Data was collected in duplicates, with both points plotted. A model was fit through this data to enable prediction of expected fluorescence quenching for a given cell density on experimental data. An example of the effect of the correction (*right panel*). An mCherry expression vector induced with low (open circles) and high (closed circles) concentration arabinose is presented without (grey) and with (black) correction. Data was collected from three biological replicates and all points are plotted. **C-D. Absolute protein quantification in molecules per cell (C) and molar concentration (D).** mCherry expression (*top*) from medium (pS361, p15A) and high (pS381, colE1) copy vectors was induced at a range of arabinose concentrations and quantified in a timecourse assay in a calibrated plate reader. Data was processed as described in (A) and cell estimates based on microsphere calibrations were used to calculate per cell values (C), or OD-specific cell volume data from Volkmer et al., 2011 was used to calculate molar concentrations (D). Data was collected from three biological replicates, each of which is plotted. (*Bottom*) mCherry expression from the top panel is compared with mTagBFP2 expression from an identical assay, plotted against arabinose concentration at the 420 min post induction. Data was collected from three biological replicates. Displayed points show the mean, and error bars indicate standard deviations.

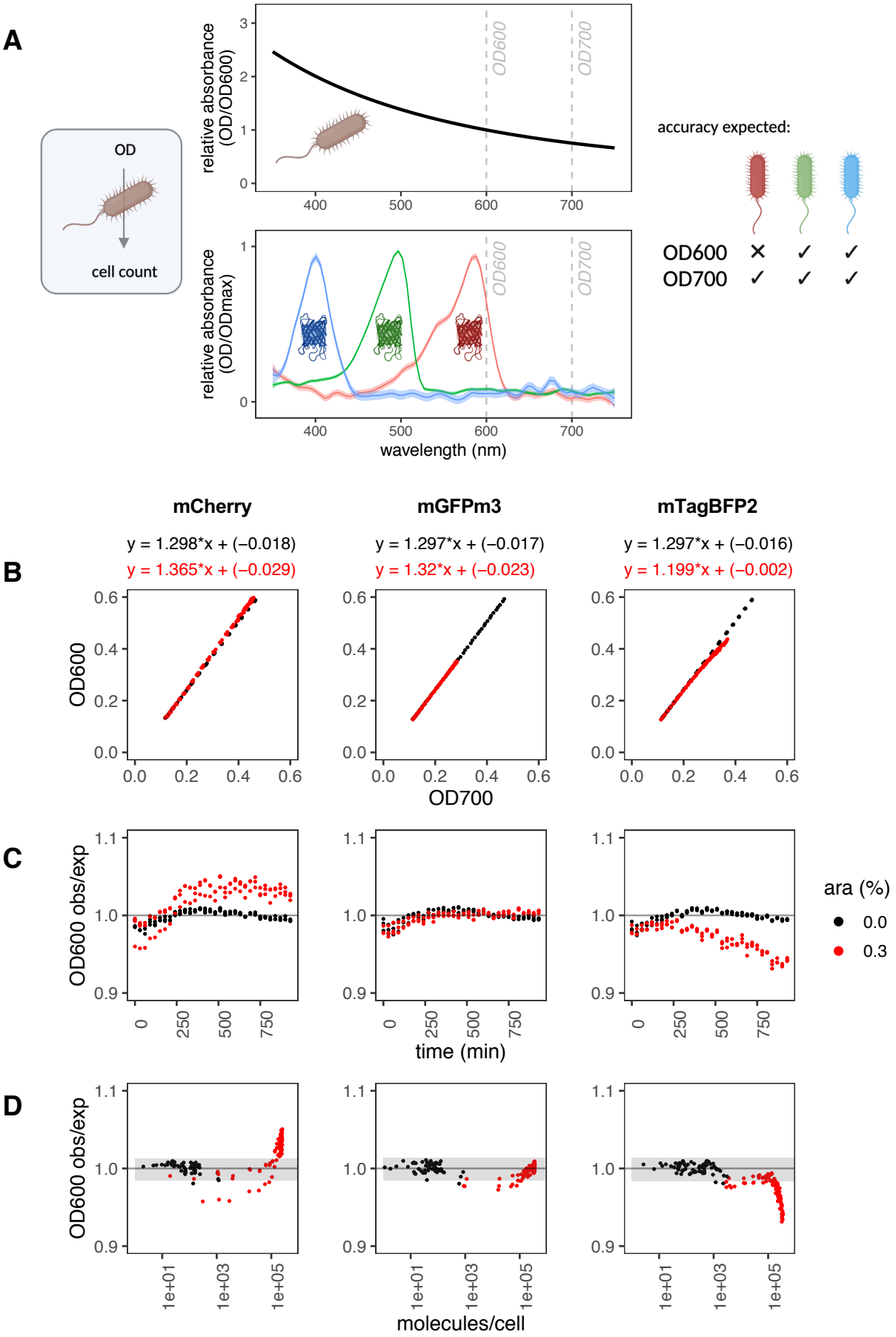
A
OD
cell count
relative absorbance (OD/OD600)
OD600
OD700
relative absorbance (OD/ODmax)
wavelength (nm)
accuracy expected:
OD600 ✕ ✓ ✓
OD700 ✓ ✓ ✓
B
mCherry
mGFPm3
mTagBFP2
y = 1.298*x + (−0.018)
y = 1.365*x + (−0.029)
y = 1.297*x + (−0.017)
y = 1.32*x + (−0.023)
y = 1.297*x + (−0.016)
y = 1.199*x + (−0.002)
OD600
OD700
C
OD600 obs/exp
time (min)
ara (%)
0.0
0.3
D
OD600 obs/exp
molecules/cell

Figure 6. Evaluation of OD600:OD700 ratios in cell growth assays.
A. Cell count accuracy with FPs. In bacterial assays, cell counts are obtained from calibrated OD600 or OD700 measurements on the assumption that the only contributor to absorbance at 600 or 700nm are cells. Cellular OD600:OD700 ratios (*top plot*, data from Supplementary Fig. 11) approximate 1.3. Red FPs like mCherry absorb light at wavelengths used for cell density assessments (*bottom plot*, data from Supplementary Fig. 1B) and may lead to an error in cell count estimates. **B-D. Timecourse expression assays of three FPs** from the pS381 vector were monitored for OD600, OD700 and fluorescence intensity every 30 minutes, without (black) and with (red) arabinose. Data was collected from three biological replicates, and all points are plotted. This is a representative experiment of at least two independent experiments for each FP. Note OD600:OD700 ratios once again approximate 1.3. **B. Relationship between OD700 and OD600 values.** Linear models were fitted to data from three FPs, and shown above each plot. **C. OD600 error plotted against time.** OD600 error was obtained by dividing observed values by expected values. Expected values were calculated from the OD700 values and the measured OD600~OD700 relationship of the 0% arabinose sample (see B). **D. Effect of FP abundance on OD600 error.** The OD600 error was plotted against abundance of each FP in molecules/cell. Grey shading indicates the mean of the samples without arabinose ± 2*standard deviations.